WIGGLERS, UNDULATORS AND THEIR APPLICATIONS

H.Onuki and P. Elleaume

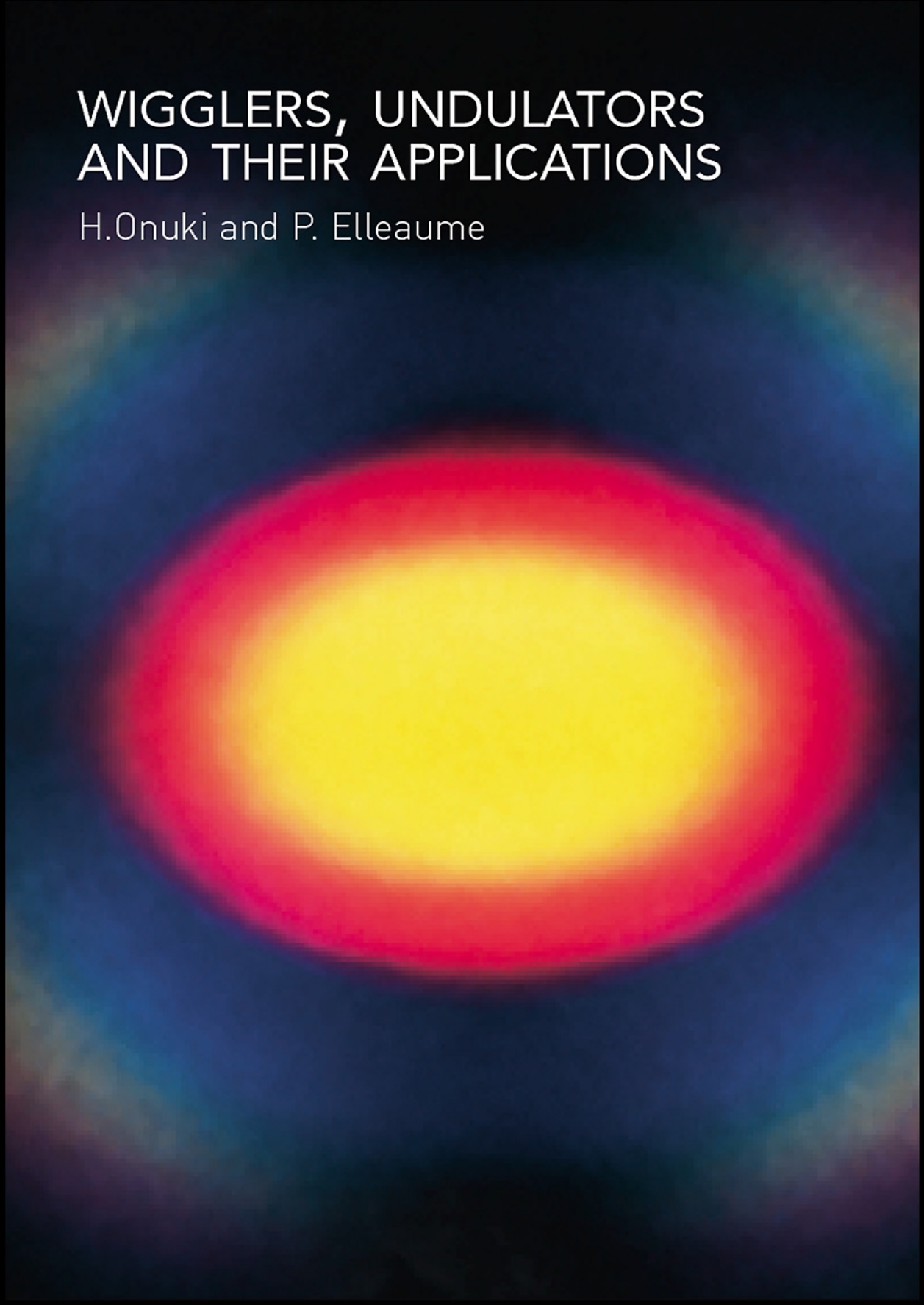

Undulators, Wigglers and their Applications

Undulators, Wigglers and their Applications

Edited by
Hideo Onuki and
Pascal Elleaume

First published 2003
by Taylor & Francis
11 New Fetter Lane, London EC4P 4EE

Simultaneously published in the USA and Canada
by Taylor & Francis Inc,
29 West 35th Street, New York, NY 10001

Taylor & Francis is an imprint of the Taylor & Francis Group

This edition published in the Taylor & Francis e-Library, 2004.

British Library Cataloguing in Publication Data
A catalogue record for this book is available from the British Library

Library of Congress Cataloging in Publication Data
A catalog record for this book has been requested

ISBN 0-203-21823-X Master e-book ISBN

ISBN 0-203-27377-X (Adobe eReader Format)
ISBN 0-415-28040-0 (Print Edition)

Contents

List of contributors vii
Preface ix

PART I
Undulators and wigglers **1**

1 Electron beam dynamics 3
LAURENT FARVACQUE

2 Generalities on the synchrotron radiation 38
PASCAL ELLEAUME

3 Undulator radiation 69
PASCAL ELLEAUME

4 Bending magnet and wiggler radiation 108
RICHARD P. WALKER

5 Technology of insertion devices 148
JOEL CHAVANNE AND PASCAL ELLEAUME

6 Polarizing undulators and wigglers 214
HIDEO ONUKI

7 Exotic insertion devices 237
SHIGEMI SASAKI

8 Free electron lasers 255
MARIE-EMMANUELLE COUPRIE

PART II
Applications **291**

9 Impact of insertion devices on macromolecular crystallography 293
SOICHI WAKATSUKI

10 Medical applications – intravenous coronary angiography as an example 322
W.-R. DIX

11 Polarization modulation spectroscopy by polarizing undulator 336
HIDEO ONUKI, TORU YAMADA AND KAZUTOSHI YAGI-WATANABE

12 Solid state physics 349
TSUNEAKI MIYAHARA

13 X-ray crystal optics 369
WAH-KEAT LEE, PATRICIA FERNANDEZ AND DENNIS M. MILLS

14 Metrological applications 421
TERUBUMI SAITO

Index 435

Contributors

Joel Chavanne is at the European Synchrotron Radiation Facility, Grenoble.

Marie-Emmanuelle Couprie is at the LURE (and CED/DSM/DRECAM), Orsay.

W.-R. Dix is at HASYLAB at DESY, Hamburg.

Pascal Elleaume is at the European Synchrotron Radiation Facility, Grenoble.

Laurent Farvacque is at the European Synchrotron Radiation Facility, Grenoble.

Patricia Fernandez is at the Advanced Photon Source, Argonne National Laboratory, Argonne.

Wah-Keat Lee is at the Advanced Photon Source, Argonne National Laboratory, Argonne.

Dennis M. Mills is at the Advanced Photon Source, Argonne National Laboratory, Argonne.

Tsuneaki Miyahara is at the Department of Physics, Tokyo Metropolitan University, Tokyo.

Hideo Onuki is at the National Institute of Advanced Industrial Science and Technology (the former Electrotechnical Laboratory), Ibaraki.

Terubumi Saito is at the National Institute of Advanced Industrial Science and Technology (the former Electrotechnical Laboratory), Ibaraki.

Shigemi Sasaki is at the Advanced Photon Source, Argonne National Laboratory, Argonne.

Soichi Wakatsuki is at the Institute of Materials Structure Science, High Energy Accelerator Research Organization, Ibaraki.

Richard P. Walker is at Diamond Light Source Ltd, Rutherford Appleton Laboratory, Oxfordshire.

Kazutoshi Yagi-Watanabe is at the National Institute of Advanced Industrial Science and Technology (the former Electrotechnical Laboratory), Ibaraki.

Toru Yamada is at the National Institute of Advanced Industrial Science and Technology (the former Electrotechnical Laboratory), Ibaraki.

Preface

When a charged particle is subjected to acceleration, it shakes off to radiate an electromagnetic field. If the acceleration is produced by a magnetic field, the radiation is called synchrotron radiation (SR). SR is the intense radiation over a broad spectral range produced by electrons or positrons in a bending magnet of a synchrotron or storage ring. In contrast to the SR produced in a uniform magnetic field, the spectral range can be concentrated around a few frequencies by "wiggling" the electron (or positron) beam. The device used to produce this effect was originally called a *wiggler*. Many short amplitude wiggles in succession serve to concentrate the radiation spatially in a narrow cone, and spectrally in a narrow frequency interval. Such a multi-period wiggler is called an *undulator*, a term introduced by H. Motz in 1951. The earliest consideration of undulators goes back to a theoretical paper written by V. L. Gintzburg in 1947. In 1953, Motz and co-workers constructed the first undulator, which was aimed at millimeter- and submillimeter-wave generation, and they succeeded in producing radiation up to the visible region. Undulator and wiggler devices are inserted in a free straight section of a storage ring and are, therefore, generically known as *Insertion Devices*.

The magnetic field produced by undulators consists of many short periods in which the angular excursion of the electron beam is of the order of the natural emission angle of the synchrotron radiation (given by $\gamma^{-1} = m_0c^2/E$, the ratio of the electron rest mass energy to its total energy). Therefore, the radiation produced in each period interferes, resulting in a spectral density that grows proportionally to the square of the number of periods, N^2, at some particular resonant frequencies and in a narrow cone of emission $N^{-1/2}$ smaller than the natural emission angle γ^{-1}. The word "wiggler" now designates a device very similar to an undulator. The difference is that a wiggler has a higher field and longer period, resulting in a larger angular excursion and a lack of phase coherence of the radiation produced in two consecutive periods (essentially due to electron beam size and divergence). A consequence of the lack of interference effects is that the spectral density of the radiation produced by a wiggler is, essentially, the sum of the spectral densities produced by each period of the magnetic fields.

Recently, there has been an increased demand for higher brilliance SR sources covering the spectral range from VUV to X-ray. The third generation of SR facilities that have already been built, or are being built, is dedicated to produce high-brilliance, high-energy radiation. These facilities are operated with ultra-low emittance electron beams and equipped with a large number of undulators and multipole wigglers installed in long straight sections. The undulators installed on the recently built high-energy rings can now produce highly brilliant X-rays. This has dramatically changed the type of science being performed with SR. More

advanced insertion devices have been developed, including polarizing undulators generating polarizing radiation of any ellipticity and other exotic insertion devices optimized for a particular application.

This volume contains a detailed presentation of the radiation produced by insertion devices, the engineering, the associated beamline instrumentation, and some scientific applications. Examples of the most important and outstanding topics have been selected from a large variety of scientific fields including that of solid state physics, biology, biomedical systems, polarization modulation spectroscopy, optical engineering and metrology. The topics are intended to stimulate the reader's interest in the many applications of insertion devices.

Because of the multidisciplinary aspect of synchrotron radiation, this book is aimed at a wide range of students, researchers and engineers working in the field of synchrotron radiation. Some background knowledge of electromagnetism and the theory of relativity will prove helpful.

Hideo Onuki
Pascal Elleaume

Part I

Undulators and wigglers

1 Electron beam dynamics

Laurent Farvacque

1 Introduction

The properties of a photon beam from a synchrotron radiation source are primarily defined by the electron beam parameters at the radiation source points, namely bending magnets or insertion devices. This chapter describes the basics of accelerator physics and points out the main parameters relevant to the use of synchrotron radiation: beam dimensions, positional stability, intensity limitations, beam lifetime etc.

We shall first describe, in Section 2, the motion of a single particle, electron or positron, along the circumference of a storage ring and check its stability conditions. We shall then consider in Section 3 a beam composed of a large number of particles. The beam dimensions in space and time will be deduced from the statistical distributions on the particles.

In Section 4 we shall look at the various unavoidable imperfections on a real accelerator and see how they affect the predictions of the previous theory.

Then, when increasing the beam intensity, and therefore the particle density, we shall be confronted with intensity limitations resulting from the interaction between the particles and their environment.

Finally, we shall identify some causes of particle losses, resulting in the finite lifetime of the particle beam.

2 Equations of motion

Generally speaking the motion of an electron (or positron) in an electromagnetic field is governed by the Lorentz equation:

$$\frac{\mathrm{d}\vec{p}}{\mathrm{d}t} = e(\vec{E} + \vec{\beta}c \times \vec{B}) \tag{1}$$

with e the charge of the particle, c the velocity of light, $\vec{R}$ the position of the particle, $\dot{\vec{R}} = \vec{\beta}c$ the velocity of the particle and $\vec{p} = m\gamma\dot{\vec{R}} = m\gamma\vec{\beta}c$ the momentum of the particle. With this single tool we want to guide the particles on a well defined closed trajectory and give them back the energy which is radiated. In a pure magnetic field ($\vec{E} = 0$) the energy variation is null. On the other hand, in the energy range of interest for synchrotron radiation, the magnetic force $e\vec{\beta}c \times \vec{B}$ is much stronger than the electric force $e\vec{E}$. We shall therefore use:

- magnetostatic fields for guiding the particles along the desired trajectory;
- electric fields for acceleration.

2.1 Reference frame

The simplest magnetic structure used in guiding a particle is a uniform magnetic field. The trajectory is then an arc of a circle with radius

$$\rho = \frac{p}{eB} \tag{2}$$

In the case of storage rings, the motion will then be studied for small deviations from a reference trajectory defined by a succession of:

- straight sections (no magnetic field);
- arcs of a circle defined by bending magnets.

The coordinate system used in the following refers to a reference particle with the nominal momentum p_0 travelling along this trajectory. Figure 1.1 shows the conventional orientation of the axis.

When studying particle dynamics one usually also refers to the phase space defined by the position $\vec{R}$ of a particle and its momentum $\vec{p}$. In accelerator jargon these are replaced by the following set of coordinates in the local system:

$$\left(x, x' = \frac{\mathrm{d}x}{\mathrm{d}s}, z, z' = \frac{\mathrm{d}z}{\mathrm{d}s}\right)$$

2.2 Equations of motion

The description of the motion can be simplified by assuming the following conditions:

1 The trajectories have small deviations from the reference particle: x and z are small; the transverse velocities v_x and v_z are small compared to the longitudinal velocity v_s; the momentum p deviates slightly from the nominal value p_0. This condition is easily verified considering the dimensions of synchrotron radiation sources.

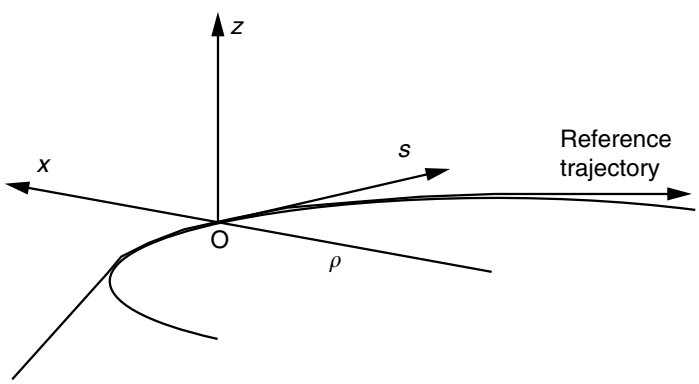

Figure 1.1 Coordinate system.

2 No acceleration – we assume that there is no energy loss due to radiation, and no accelerating electric field:

p is constant,

$v_x^2 + v_z^2 + v_s^2 = v^2$ is constant.

3 Anti-symmetric magnetic field:

$$B_x(x, z, s) = -B_x(x, -z, s)$$
$$B_z(x, z, s) = B_z(x, -z, s)$$
$$B_s(x, z, s) = -B_s(x, -z, s)$$

This condition is verified for planar horizontal machines with a mid-plane symmetry.

Within the conditions 1 and 3, the magnetic field can be expanded in a Taylor series up to the second order in the vicinity of the reference trajectory. The normalisation with respect to the momentum is introduced by defining the following quantities:

$$\begin{aligned} h &= \frac{B_0}{p_0/e} && \text{curvature of the reference trajectory} \\ k &= \frac{\partial B_z/\partial x}{p_0/e} && \text{normalised field gradient} \\ m &= \frac{1}{2}\frac{\partial^2 B_z/\partial x^2}{p_0/e} && \text{normalised field second derivative} \end{aligned} \tag{3}$$

We obtain the field expansion up to the second order in x and z:

$$\begin{aligned} \frac{B_x}{p_0/e} &= kz + 2mxz + \cdots \\ \frac{B_z}{p_0/e} &= h + kx + mx^2 - \frac{1}{2}(h'' + hk + 2m)z^2 + \cdots \\ \frac{B_s}{p_0/e} &= h'z + (k' - hh')xz + \cdots \end{aligned} \tag{4}$$

where the $'$ denotes differentiation with respect to s.

The equation of motion in the laboratory frame, expressed in the local axis system is:

$$\begin{aligned} x'' - h(1 + hx) - x'(hx' + h'x) &= \frac{e}{p}\sqrt{x'^2 + z'^2 + (1 + hx)^2}\,[z'B_s - (1 + hx)B_z] \\ z'' - z'(hx' + h'x) &= \frac{e}{p}\sqrt{x'^2 + z'^2 + (1 + hx)^2}\,[(1 + hx)B_x - x'B_s] \end{aligned} \tag{5}$$

Considering condition 1, we introduce the momentum deviation $\delta = (p - p_0)/p_0 \ll 1$. Combining equations (4) and (5) and using $p_0/p = 1/(1 + \delta) \approx 1 - \delta + \delta^2$ we obtain the

development of the equations of motion to the second order:

$$\begin{aligned} x'' + (h^2 + k)x &= h\delta - (2hk + m + h^3)x^2 + h'xx' + \tfrac{1}{2}hx'^2 + (2h^2 + k)x\delta \\ &\quad + \tfrac{1}{2}(h'' + hk + 2m)z^2 + h'zz' - \tfrac{1}{2}hz'^2 - h\delta^2 + \cdots \\ z'' - kz &= 2(m + hk)xz + h'xz' - h'x'z + hx'z' - kz\delta + \cdots \end{aligned} \tag{6}$$

We shall now introduce two additional simplifications:

- we restrict ourselves to perfect 'hard edged' magnetic elements, where the field does not depend on s, so that we have $h' = h'' = 0$;
- we keep only the first order in x and z.

The equation of motion then takes the simple form:

$$\begin{cases} x'' + K_x^2 x = h\delta & \text{with } K_x^2 = h^2 + k \\ z'' + K_z^2 z = 0 & \text{with } K_z^2 = -k \end{cases} \tag{7}$$

Motions in the horizontal and vertical planes are independent. If we first look at the horizontal motion, the solution depends on the sign of K_x^2:

1 $K_x^2 > 0,\ k_x = \sqrt{K_x^2}$
The equation without the right-hand side ($\delta = 0$, the particle has the nominal momentum) describes a harmonic oscillator. Its solution is of the form $x = A\cos(k_x s) + B\sin(k_x s)$. Consequently we have $x' = -Ak_x \sin(k_x s) + Bk_x \cos(k_x s)$ and the constants A and B can be obtained from the initial conditions $s = 0$, $x = x_0$, $x' = x'_0$. This gives $A = 1$ and $B = 1/k_x$. After including the term on the right-hand side, the motion can be written as

$$\begin{pmatrix} x \\ x' \end{pmatrix} = \begin{pmatrix} \cos(k_x s) & 1/k_x \sin(k_x s) \\ -k_x \sin(k_x s) & \cos(k_x s) \end{pmatrix} \cdot \begin{pmatrix} x_0 \\ x'_0 \end{pmatrix} + \begin{pmatrix} h/k_x^2(1 - \cos(k_x s)) \\ h/k_x \sin(k_x s) \end{pmatrix} \cdot \delta \tag{8}$$

2 $K_x^2 < 0,\ k_x = \sqrt{-K_x^2}$
A similar solution gives

$$\begin{pmatrix} x \\ x' \end{pmatrix} = \begin{pmatrix} \cosh(k_x s) & 1/k_x \sinh(k_x s) \\ k_x \sinh(k_x s) & \cosh(k_x s) \end{pmatrix} \cdot \begin{pmatrix} x_0 \\ x'_0 \end{pmatrix} + \begin{pmatrix} h/k_x^2(\cosh(k_x s) - 1) \\ h/k_x \sinh(k_x s) \end{pmatrix} \cdot \delta \tag{9}$$

3 $K_x^2 = 0$
The solution is simply

$$\begin{pmatrix} x \\ x' \end{pmatrix} = \begin{pmatrix} 1 & s \\ 0 & 1 \end{pmatrix} \cdot \begin{pmatrix} x_0 \\ x'_0 \end{pmatrix} + \begin{pmatrix} hs^2/2 \\ hs \end{pmatrix} \cdot \delta \tag{10}$$

A similar resolution may be applied to the vertical motion. The motion in each plane can be described by the matrix expression:

$$\mathbf{X} = \mathbf{T} \cdot \mathbf{X_0} + \mathbf{D} \cdot \delta \tag{11}$$

where $\mathbf{X}$ is the particle coordinate vector,

$$\mathbf{X} = \begin{pmatrix} x \\ x' \end{pmatrix}$$

and $\mathbf{T}$, the 'transfer matrix', has the form

$$\mathbf{T} = \begin{pmatrix} t_{11} & t_{12} \\ t_{21} & t_{22} \end{pmatrix}$$

and the property

$$\det(\mathbf{T}) = 1 \tag{12}$$

2.3 Magnetic lattice

The desired properties of a storage ring are achieved by aligning on the reference trajectory a succession of such magnetic elements, usually separating the different functions of bending and focusing. These elements are:

Drift space: $h = 0, k = 0, m = 0$
No magnetic field.

Dipole: $h = \text{constant}, k = 0, m = 0$
The dipole bends the trajectory with a constant radius. Expression (7) also shows that it gives focusing in the horizontal plane and is equivalent to a drift space in the vertical plane. Additional focusing may be obtained by inclining the dipole entrance and exit faces with respect to the plane perpendicular to the reference trajectory (Figure 1.2).

Quadrupole: $h = 0, k = \text{constant}, m = 0$
Such an element gives focusing in one plane and defocusing in the other plane. Alternating focusing and defocusing quadrupoles produces focusing in both planes (Figure 1.3).

Sextupole: $h = 0, k = 0, m = \text{constant}$
This element is equivalent to a drift space at the first order but is used for higher order corrections.

It is also possible to design combined function magnets, for instance, bending + focusing (dipole magnet with field index), or focusing + sextupolar strength.

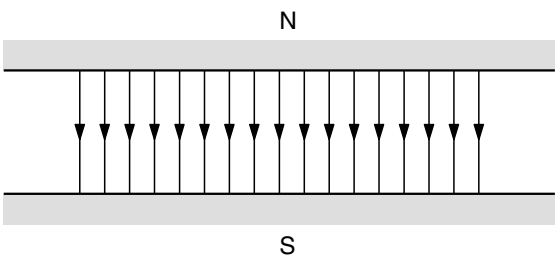

Figure 1.2 Dipolar field.

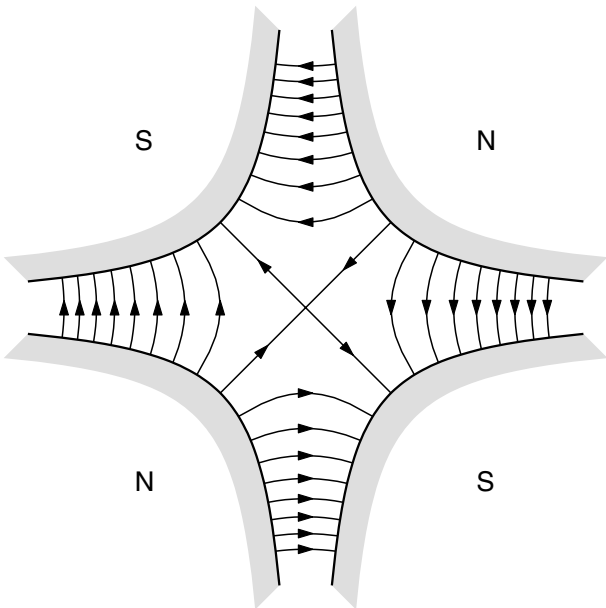

Figure 1.3 Quadrupolar field.

3 Single particle motion

3.1 Transverse motion

We shall first look at the case $\delta = 0$. The differential equations (7) are then similar for both the horizontal and vertical planes, and the solution developed for the horizontal plane also applies in the vertical plane. A storage ring is made up of several identical sequences of magnetic elements called superperiods. As we want the particle to circulate indefinitely in the ring we must now state that K_x^2 and K_z^2 in Eqn (7) are periodic functions of s with period S, length of the machine's superperiod. Such a system is known as Hill's equation. Starting from an arbitrary origin on the circumference, one can build the transfer matrix corresponding to one superperiod, obtained by multiplying all the single element matrices:

$$\mathbf{T} = \mathbf{T}_n \cdot \mathbf{T}_{n-1} \cdots \mathbf{T}_2 \cdot \mathbf{T}_1$$

3.1.1 β-functions

Now, one has to find conditions for which the motion over n turns is bound. This is usually expressed by writing for each plane the 2×2 transfer matrix of one superperiod in the general Twiss form, which results from $\det(\mathbf{T}) = 1$:

$$\mathbf{T} = \begin{pmatrix} t_{11} & t_{12} \\ t_{21} & t_{22} \end{pmatrix} = \begin{pmatrix} \cos\mu + \alpha \sin\mu & \beta \sin\mu \\ -\gamma \sin\mu & \cos\mu - \alpha \sin\mu \end{pmatrix} \tag{13}$$

The stability condition is then given by μ real, or $\cos\mu = \frac{1}{2}(t_{11} + t_{22}) < 1$; μ does not depend on the choice of the origin. On the other hand α, β, γ are periodic functions of s with period S (length of the superperiod) and with the properties $\beta\gamma - \alpha^2 = 1$ and $\alpha = -\beta'/2$.

3.1.2 Betatron oscillations

If the stability condition is fulfilled, two independent solutions of the equations of motion are

$$\begin{aligned} C(s) &= \sqrt{\beta(s)}\cos(\varphi(s)) \\ S(s) &= \sqrt{\beta(s)}\sin(\varphi(s)) \end{aligned} \tag{14}$$

where the function φ is defined by $\varphi(s) = \int_s \mathrm{d}s/\beta(s)$ and is called the 'betatron phase advance'.

The trajectory of any particle can be written as a linear combination of these two trajectories: $x(s) = c \cdot C(s) + s \cdot S(s) \cdot x'$ is obtained by differentiation and the trajectory can be written in the form:

$$\begin{pmatrix} x/\sqrt{\beta} \\ (\alpha x + \beta x')/\sqrt{\beta} \end{pmatrix} = \begin{pmatrix} \cos\varphi & \sin\varphi \\ -\sin\varphi & \cos\varphi \end{pmatrix} \cdot \begin{pmatrix} c \\ s \end{pmatrix} \tag{15}$$

The constants c and s are given by the initial conditions $s = 0$, $x = x_0$, $x' = x'_0$. The motion along s is a pseudo-harmonic oscillation around the reference trajectory, with local peak amplitude of the oscillation proportional to $\sqrt{\beta(s)}$. This motion can be turned into a simple harmonic oscillation by changing the variables s into $\varphi(s)$, x into $X = x/\sqrt{\beta}$ and x' into $X' = \mathrm{d}X/\mathrm{d}\varphi = (\alpha x + \beta x')/\sqrt{\beta}$.

As a consequence, we have, all along the trajectory, $X^2 + X'^2 = \text{constant}$, or in the initial coordinate system

$$\gamma x^2 + 2\alpha x x' + \beta x'^2 = \varepsilon = \text{constant} \tag{16}$$

This constant ε is called the Courant–Snyder invariant of the particle.

3.1.3 Tunes

Since $\beta(s)$ is periodic, the phase advance over one superperiod $\varphi(s+S) - \varphi(s)$ is independent of the choice of the origin s. From the definitions of μ and $\varphi(s)$ it appears that $\mu = \varphi(S)$: μ is the phase advance per superperiod. This leads to the definition of the tune ν so that $N\mu = 2\pi\nu$, N being the number of superperiods in the machine, ν the number of betatron oscillations per turn. Following Eqn (16), the position x_n of a particle in phase space, at turn n, at a given location around the circumference satisfies the relation:

$$\gamma x_n^2 + 2\alpha x_n x'_n + \beta x'^2_n = \varepsilon = \text{constant} \tag{17}$$

In the phase space (x, x') corresponding to the chosen origin, the particle describes the ellipse shown in Figure 1.4. The Twiss parameters α, β, γ describe the orientation this ellipse while $\pi\varepsilon$ is its surface. The particle horizontal x position seen at this location samples at the revolution frequency ω_0 an oscillation with a frequency $\omega_\beta = \nu \cdot \omega_0$ called the 'betatron oscillation'.

3.1.4 Dispersion

We consider now the case of a particle with δ (momentum deviation) non-zero and constant. There is one particular solution of Eqn (7) so that the position and angle after one superperiod are equal to the initial values. This is obtained by solving the system:

$$(\mathbf{T} - \mathbf{I}) \cdot \mathbf{X} = -\mathbf{D} \cdot \delta \tag{18}$$

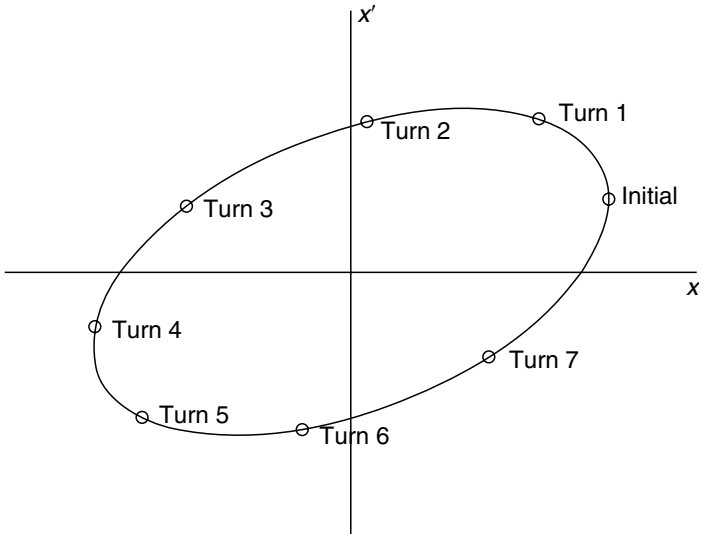

Figure 1.4 Betatron motion.

where **I** is the identity matrix. The solution is proportional to δ. The periodic trajectory corresponding to $\delta = 1$ is called the 'dispersion', the components of which are $\eta(s)$, $\eta'(s)$. The trajectory of any particle can then be written as the sum of the general solution of the homogeneous equation plus the dispersion:

$$x(s) = c \cdot \sqrt{\beta(s)} \cos(\varphi(s)) + s \cdot \sqrt{\beta(s)} \sin(\varphi(s)) + \delta \cdot \eta(s) \tag{19}$$

The off-momentum particle describes the betatron pseudo-periodic oscillation, with the amplitude modulated like $\sqrt{\beta(s)}$, around the periodic off-momentum orbit $\delta \cdot \eta(s)$. The constants c, s, δ are again defined by the initial conditions.

3.2 Longitudinal motion

We now look at the acceleration process: in the case of a synchrotron radiation source, it must compensate for energy losses due to radiation. Acceleration is provided by a longitudinal time varying electric field. The definition of the reference particle can be extended by stating that for each revolution (along the reference trajectory) it has to cross the accelerating gap at a time when the voltage compensates exactly the average energy loss per turn. This implies that the voltage frequency must be a multiple h of the particle revolution frequency, and can be written as

$$V = \hat{V} \sin(h\omega_0 t + \phi_s) \tag{20}$$

with $\omega_0 = 2\pi f_0 = \beta c/R$ the revolution angular frequency, $R = C/2\pi$ the machine radius and h the harmonic number. The phase shift ϕ_s of the reference particle with respect to the voltage is imposed by the peak voltage and the average energy loss per turn ΔE.

$$\Delta E = e\hat{V} \sin \phi_s \tag{21}$$

The test particle can again be described by its deviations from the reference particle: momentum deviation δ and phase deviation $\Delta\phi$.

3.2.1 Momentum compaction factor

By definition, the momentum compaction α_C relates the orbit length of a particle to its momentum deviation:

$$\alpha_C = \frac{dC/C}{\delta} \tag{22}$$

This is a geometric factor related to the dispersion function introduced in Eqn (18):

$$\alpha_C = \frac{1}{C}\int_C \frac{\eta}{\rho}\,ds \tag{23}$$

where ρ is the local radius of curvature of the reference trajectory.

When studying the longitudinal motion one needs to relate the period of revolution of the test particle to its momentum deviation. This is expressed by the factor η_C derived from α_C:

$$\eta_C = \frac{df/f}{\delta} = \frac{1}{\gamma^2} - \alpha_C \tag{24}$$

η_C depends on the energy of the particle but for electron machines where $\gamma \gg 1$, one often makes the approximation $\eta_C \approx -\alpha_C$.

3.2.2 Synchrotron oscillation

Over one turn, the test particle gains energy: $d(\Delta E) = e\hat{V}(\sin(\phi_s + \Delta\phi) - \sin\phi_s)$ and drifts in phase with respect to the reference particle: $d(\Delta\phi) = -2\pi h\eta_C\delta$. By dividing by the revolution period one obtains a set of two differential equations in δ and $\Delta\phi$, or, by combining both, a second order differential equation describing the motion:

$$\ddot{\Delta\phi} + \frac{\Omega_s^2}{\cos\phi_s}(\sin(\phi_s + \Delta\phi) - \sin\phi_s) = 0 \tag{25}$$

where

$$\Omega_s^2 = \frac{e\hat{V}h\omega_0\eta_C\cos\phi_s}{2\pi Rp_0}$$

Integrating Eqn (25) gives an invariant for the longitudinal motion:

$$H = \frac{\dot{\Delta\phi}^2}{2} - \Omega_s^2\frac{\cos(\phi_s + \Delta\phi) - \cos\phi_s + \Delta\phi\sin\phi_s}{\cos\phi_s} = \text{constant} \tag{26}$$

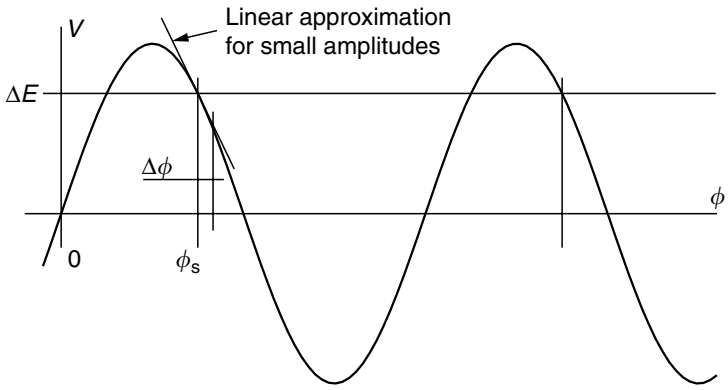

Figure 1.5 RF accelerating voltage.

For small amplitudes the differential equation of motion (25) becomes

$$\ddot{\Delta\phi} + \Omega_s^2 \Delta\phi = 0 \tag{27}$$

and an invariant of the motion is

$$H = \frac{\dot{\Delta\phi}^2}{2} + \Omega_s^2 \frac{\Delta\phi^2}{2} = \text{constant} \tag{28}$$

This can also be written as a function of δ:

$$I = \delta^2 + \frac{\Omega_s^2}{h^2 \eta_C^2 \omega_0^2} \Delta\phi^2 = \text{constant} \tag{29}$$

Again, we find a harmonic oscillation provided Ω_s^2 is positive. Ω_s, the angular frequency of small amplitude oscillations is called 'synchrotron frequency'. It is usually much smaller than the betatron frequency. As for transverse motion, the position of the particle in phase space, now using the coordinates $(\Delta\phi, \delta)$ describes an ellipse. This linear approximation is valid in the domain where one can approximate the sinusoidal RF voltage (Figure 1.5) by its slope in the vicinity of the synchronous phase. On the other hand if the amplitude of oscillation increases, the non-linearities become significant and the trajectory in phase space deviates from an ellipse. Finally, one reaches a limit above which the motion becomes unstable. This separatrix defines a maximum momentum deviation δ_m from the reference ('momentum acceptance') and a maximum phase deviation ('bucket length') within which particles can be kept:

$$\delta_m = \frac{1}{\beta} \sqrt{\frac{e\hat{V} \cos\phi_s}{\pi h \eta_C E} [2 - (\pi - 2\phi_s) \tan\phi_s]} \tag{30}$$

3.3 Non-linearities

Obviously, the linear approximation of the transverse motion is valid in a limited domain: the basic equations of motion (Eqn (6)) have been arbitrarily truncated to the first order, even for

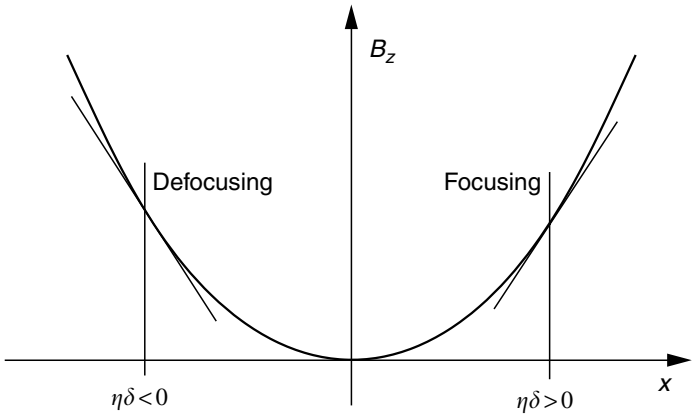

Figure 1.6 Chromaticity compensation.

the simplest magnetic elements. For larger transverse oscillation amplitudes, it is necessary to include higher orders.

3.3.1 Chromaticity

Chromaticity is a measurement of the change in focusing with momentum deviation. It is defined as the relative tune change (horizontal or vertical) per unit momentum deviation:

$$\xi_x = \frac{\Delta\nu_x/\nu_x}{\delta} \tag{31}$$

and similarly for the vertical plane. Since the tune control is crucial for the performance of a storage ring, one usually wants to minimise or at least control the chromaticity. This can be done by inserting sextupole magnets in the lattice where the dispersion is large. Figure 1.6 describes the principle of this compensation: particles with different energies oscillate about different orbits and therefore experience a different focusing strength.

3.3.2 Dynamic acceptance

In reality, even the simplest magnets considered until now are not perfectly linear, because of their finite aperture or field imperfections. In addition non-linear magnets, such as sextupoles, are introduced on purpose so that for increasing amplitudes the motion also becomes non-linear. The betatron oscillation frequency then varies with amplitude and, as for the longitudinal direction, a maximum amplitude for stable motion may be reached. This is called the 'dynamic acceptance' of the machine. The dynamic acceptance can be optimised primarily by tuning additional sextupole magnets so that the detrimental effects of chromaticity sextupoles can be minimised.

4 Emittances

After studying the motion of a single particle, we shall now look at the behaviour of a bunch of particles. Initially we consider that there is no collective effect, meaning that each particle

behaves as if it were alone. We know that at a given location along the circumference of the storage ring the position, turn after turn, of any particle in phase space (x, x' or z, z') describes an ellipse. According to Liouville's theorem, the particle density in phase space in the vicinity of any particle is a constant, and consequently the surface enclosed in any isodensity curve is a constant. From these two statements we can deduce that any distribution whose isodensity curves are ellipses satisfying $\gamma x^2 + 2\alpha x x' + \beta x'^2 = \varepsilon$ is invariant over one or any number of turns.

4.1 Emittance, beam envelope, beam sizes

The surface enclosed in an isodensity curve being constant, it can be used as a measurement of the beam occupancy. The density level to be used as reference is arbitrary. It is customary for electron (or positron) machines to take one standard deviation of the projected distribution. In the horizontal plane, as the different energies in the bunch follow different trajectories, one has also to take into account the energy spread of the distribution σ_δ and the dispersion function η. The beam size and divergence can be deduced from Figure 1.7.

The beam envelope is entirely defined by knowing ε, σ_δ (constants) and the functions $\beta(s)$ and $\eta(s)$.

4.2 Acceptance

The emittance has been defined as the area in phase space occupied by the beam. Similarly, we define the acceptance as the area in phase space where a particle can have a stable motion. The acceptance may be limited either by the maximum stable amplitude resulting from the non-linearities – this is the dynamic acceptance defined above – or by the dimensions of the vacuum chamber – physical aperture. The acceptance plays a role in the design of the injection scheme and in the lifetime of the beam.

4.2.1 Transverse acceptance

The transverse acceptance is limited by the dimension A of the vacuum chamber (Figure 1.8). It can be quantified in each plane (horizontal or vertical) by the maximum invariant value ε_m

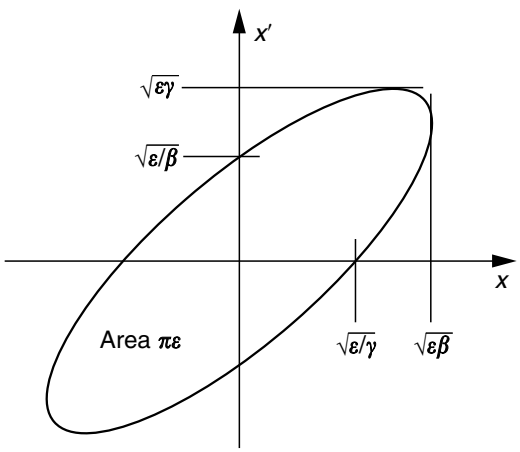

	Horizontal	*Vertical*
Size	$\sqrt{\varepsilon_x \beta_x + \eta^2 \sigma_\delta^2}$	$\sqrt{\varepsilon_z \beta_z}$
Divergence	$\sqrt{\varepsilon_x \gamma_x + \eta'^2 \sigma_\delta^2}$	$\sqrt{\varepsilon_z \gamma_z}$

Figure 1.7 Beam emittance.

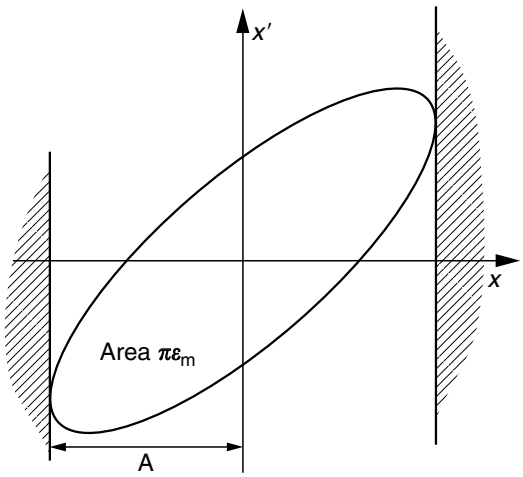

Figure 1.8 Acceptance of the vacuum chamber.

that can be kept within the chamber over an infinite number of turns.

$$\varepsilon_{\mathrm{m}} = \min_{\text{Circumference}} \left(\frac{A^2_{\text{chamber}}}{\beta} \right) \tag{32}$$

4.2.2 Longitudinal acceptance

The longitudinal acceptance is limited for two reasons: as shown in Section 3.2.2, the momentum deviation is limited by the RF system (Eqn (30)), but as off-momentum particles follow off-centred trajectories it may also be limited by the horizontal aperture of the machine:

$$\delta_{\mathrm{m}} = \min_{\text{Circumference}} \left(\frac{A_{\text{chamber}}}{|\eta|} \right) \tag{33}$$

This defines the longitudinal acceptance for particles without betatron oscillations. The momentum acceptance in case of sudden momentum jumps is further reduced by the fact that a momentum jump also induces a correlated betatron oscillation if the dispersion is non-zero. The momentum acceptance now depends on the location of the momentum jump. Equation (33) has to be modified to include the betatron oscillation, and the set of equations defining the momentum acceptance becomes:

$$\begin{cases} \delta_{\mathrm{m}} = \min\limits_{\text{Circumference}} \left(\dfrac{A_{\text{chamber}}}{|\eta| + \sqrt{\beta H^*}} \right) \\ \delta_{\mathrm{m}} = \dfrac{1}{\beta} \sqrt{\dfrac{e\hat{V} \cos \phi_{\mathrm{s}}}{\pi h \eta_{\mathrm{C}} E}} [2 - (\pi - 2\phi_{\mathrm{s}}) \tan \phi_{\mathrm{s}}] \end{cases} \tag{34}$$

where the function H is defined by:

$$H = \gamma_x \eta^2 + 2\alpha_x \eta\eta' + \beta_x \eta'^2$$

and the * denotes the value of the function H at the location of the momentum jump.

4.3 Radiation excitation/damping

In addition to the interactions studied until now, the particles emit photons. The theory of synchrotron radiation will be detailed in Chapter 2 but as far as the electron motion is concerned, we shall assume now that the electron may randomly be subjected to a sudden momentum change corresponding to the energy given to the emitted photon. This implies a change of the invariants of the particle. A momentum kick $\Delta\delta$ induces a change ΔI in the longitudinal invariant I defined in Eqn (29):

$$\Delta I = 2\delta \cdot \Delta\delta + \Delta\delta^2 \tag{35}$$

It also induces a change of the horizontal invariant because the reference trajectory is different for different energies where the dispersion is non-zero:

$$\Delta\varepsilon_x = -2\left[\gamma_x x\eta + \alpha_x (x\eta' + x'\eta) + \beta_x x'\eta'\right]\Delta\delta + \left[\gamma_x \eta^2 + 2\alpha_x \eta\eta' + \beta_x \eta'^2\right]\Delta\delta^2 \tag{36}$$

As the photon emission is not exactly collinear with the electron trajectory, the particle may in addition experience a horizontal kick $\Delta x'$ resulting also in a change of horizontal invariant:

$$\Delta\varepsilon_x = 2(\alpha_x x + \beta_x x')\Delta x' + \beta_x \Delta x'^2 \tag{37}$$

This last effect happens similarly in the vertical plane.

On the other hand, the acceleration in RF cavities necessary to compensate for losses will restore momentum in the longitudinal direction only. Therefore, it has a damping effect on transverse oscillations. Because of all these invariant changes, the particle distribution in phase space may vary with time. The evolution of the particle distribution $w(\varepsilon, t)$ is governed by the Fokker–Planck equation:

$$\frac{\partial w}{\partial t} = -\frac{\partial}{\partial \varepsilon}(wA_1) + \frac{1}{2}\frac{\partial^2}{\partial \varepsilon^2}(wA_2) \tag{38}$$

with

$$A_1 = \lim_{\delta t \to 0} \frac{\langle \delta\varepsilon \rangle}{\delta t} \quad \text{and} \quad A_2 = \lim_{\delta t \to 0} \frac{\langle \delta\varepsilon^2 \rangle}{\delta t}$$

We look for a stationary distribution of particles. Knowing the properties of synchrotron radiation emission we can compute A_1 and A_2 and look for the condition $\partial w/\partial t = 0$.

4.4 Equilibrium emittances

The average linear and quadratic invariant changes per unit time (A_1 and A_2) can be expressed as functions of a few integrals of the machine functions:

$$I_2 = \oint_C \frac{1}{\rho^2}\,\mathrm{d}s \qquad I_3 = \oint_C \frac{1}{|\rho|^3}\,\mathrm{d}s \qquad I_4 = \oint_C \frac{(1-2n)\eta}{\rho^3}\,\mathrm{d}s$$

$$I_5 = \oint_C \frac{\gamma_x\eta^2 + 2\alpha_x\eta\eta' + \beta_x\eta'^2}{|\rho|^3}\,\mathrm{d}s \qquad I_z = \oint_C \frac{\beta_z}{|\rho|^3}\,\mathrm{d}s$$

The average values for the energy loss and radiated power are

$$\Delta E = \tfrac{2}{3} r_\mathrm{e} mc^2 \beta^3 \gamma^4 I_2 \quad \text{(average energy loss per turn)} \tag{39}$$

where r_e is the classical electron radius, $r_\mathrm{e} = 2.82 \cdot 10^{-15}$ m, or in more practical units

$$\Delta E = \frac{C_\gamma E^4}{2\pi} I_2 \tag{40}$$

with $C_\gamma = (4\pi/3)(r_\mathrm{e}/E_0^3) = 8.8575 \cdot 10^{-5}\,\mathrm{m/GeV^3}$.

We then obtain for each phase space distribution (horizontal, vertical, longitudinal) a damping time and an equilibrium distribution. Starting with the definition of damping partition numbers

$$J_x = 1 - I_4/I_2 \qquad J_z = 1 \qquad J_\delta = 2 + I_4/I_2 \tag{41}$$

The damping times are

$$\tau_i = \frac{4\pi T_0}{J_i C_\gamma E^3 I_2} \qquad i = x, z, \delta \tag{42}$$

Horizontally, the contribution of the photon emission angle (Eqn (37)) can be neglected compared to the contribution of energy/dispersion (Eqn (36)) to the invariant growth.

The horizontal emittance is

$$\varepsilon_x = C_\mathrm{q} \frac{\gamma^2}{J_x} \frac{I_5}{I_2} \tag{43}$$

with $C_\mathrm{q} = \frac{55}{32\sqrt{3}}(\hbar c/mc^2) = 3.84 \cdot 10^{-13}$ m.

Vertically, the only excitation comes from the photon emission angle. Usual values of vertical equilibrium emittance are so small that it can be neglected.

$$\varepsilon_z = C_\mathrm{q} \frac{1}{J_z} \frac{I_z}{I_2} \quad \text{(vertical emittance)} \tag{44}$$

$$\sigma_\delta = \sqrt{C_\mathrm{q} \frac{\gamma^2}{J_\varepsilon} \frac{I_3}{I_2}} \quad \text{(momentum spread)} \tag{45}$$

$$\sigma_s = \frac{\beta c |\eta_\mathrm{C}|}{\Omega_\mathrm{s}} \sigma_\delta \quad \text{(bunch length)} \tag{46}$$

4.5 Time structure

Following Eqn (46) the beam intensity has a Gaussian shape, with a standard deviation in time σ_τ given by:

$$\sigma_\tau = \frac{\sigma_s}{\beta c} = \frac{|\eta_C|}{\Omega_s}\sigma_\delta \tag{47}$$

The maximum repetition rate is defined by the harmonic number h chosen for the RF system and is obtained when all the available buckets are filled. This so-called 'multibunch operation' gives the maximum average intensity. At the other extreme, a minimum repetition rate may be achieved by filling only one of the buckets: this is the 'single bunch operation', providing the maximum peak intensity and giving the possibility of time-resolved experiments. In between, any filling pattern may be envisaged to reach a compromise between average intensity and time resolution. The repetition frequency is chosen between the two extreme cases:

$$\begin{aligned} \omega_{\min} &= \omega_0 = \frac{\beta c}{R} \\ \omega_{\max} &= h\omega_0 \end{aligned} \tag{48}$$

4.6 Matching of β functions

The previous equations set up the main constraints for the design of synchrotron radiation sources:

- The horizontal β-function and the dispersion must be optimised to reduce the integral I_5 and therefore the horizontal emittance. A basic feature is a small β_x value in the dipoles, where radiation occurs.
- The energy spread cannot be varied significantly for a given bending radius, but the bunch length can be modified through optics tuning (η_C) or RF parameters (Ω_s).
- Dipole field index n allows modifying the sharing of emittances and damping times between horizontal and longitudinal directions through the integral I_4.

In addition, the β-function in both planes can be matched at the radiation source points to best fit the photon beam users. The emittance of the photon beam is the convolution of the single electron photon emission (fixed) and the electron beam emittance (tuneable). For a given emittance value the ratio size/divergence (equal to β) can be chosen so that:

- If the emittance is larger than the diffraction limit, the single electron emission can be neglected and the minimum size on the sample (without focusing) calls for large β values (of the order of the distance from the source to the sample). Focusing the electron beam downstream the beamline could even give smaller spot sizes. Minimising the width of harmonics also calls for a large horizontal β (or small angular divergence).
- If the electron beam emittance approaches the diffraction limit, the spot size becomes independent of the electron optics. Maximum brightness is then achieved when the electron and diffraction emittances are matched. This corresponds to small β values (half the undulator length). This applies to the vertical plane where the emittance is naturally small and also horizontally when the photon beam is focused on the beamline.

These conditions have led to a few basic lattice design.

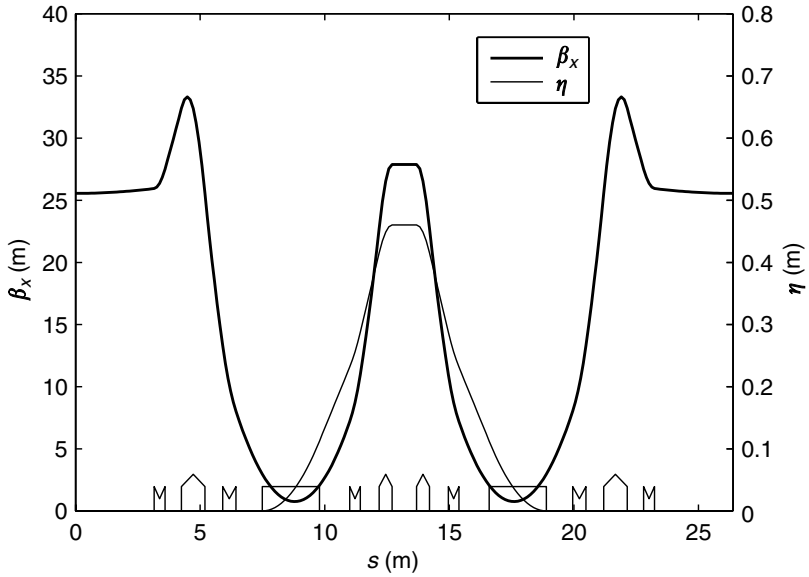

Figure 1.9 Expanded Chasman–Green lattice.

4.6.1 Double bend achromat

The Chasman–Green lattice is a compact lattice set to have zero dispersion in the straight sections, for minimising the beam size. Figure 1.9 shows the horizontal β-function and dispersion. The theoretical minimum emittance of such a lattice can be computed. Equation (49) gives the value in the simple case where all the bending magnets are identical:

$$\varepsilon_x = \frac{C_q \gamma^2}{4\sqrt{15} J_x} \left(\frac{2\pi}{N_{\text{mag}}} \right)^3 \tag{49}$$

The theoretical minimum emittance scales with the third power of the deflection angle of one bending magnet: increasing the number of superperiods and consequently the machine length reduces the emittance. If the condition of zero dispersion is relaxed, the theoretical minimum emittance is even smaller:

$$\varepsilon_x = \frac{C_q \gamma^2}{12\sqrt{15} J_x} \left(\frac{2\pi}{N_{\text{mag}}} \right)^3 \tag{50}$$

However, the beam size in the straight sections now depends on the energy spread of the beam and on the dispersion value. A compromise between dispersion and emittance has to be made to get the minimal beam size.

4.6.2 Triple bend achromat

This type of lattice, with the same constraint of zero dispersion in the straight sections has a slightly smaller emittance than the Chasman–Green lattice: it is given by Eqn (51) for

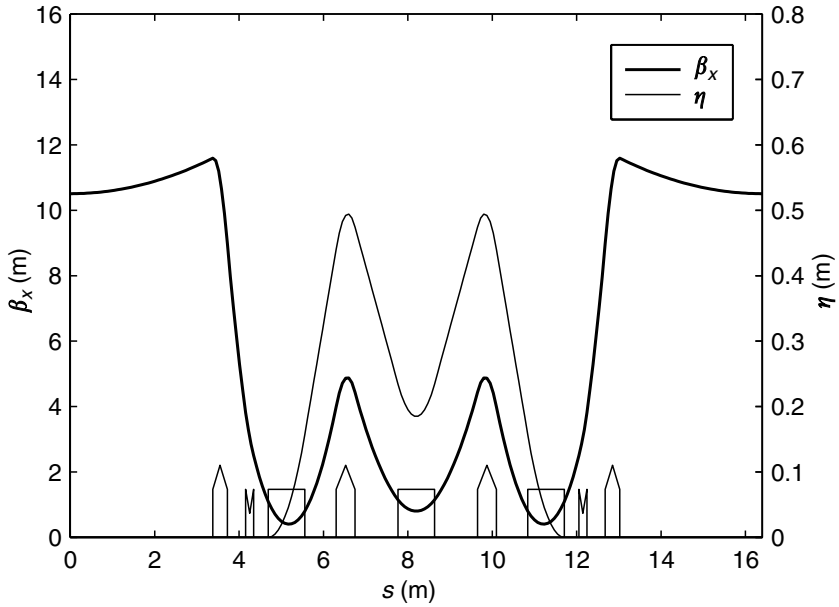

Figure 1.10 Triple bend achromat lattice.

identical bending magnets. Its β-function and dispersion are plotted in Figure 1.10.

$$\varepsilon_x = \frac{7C_q\gamma^2}{36\sqrt{15}J_x}\left(\frac{2\pi}{N_{\text{mag}}}\right)^3 \tag{51}$$

However, for technical reasons the emittance for realistic lattice designs is always much larger than the theoretical optimum, and the choice of the lattice is governed by many other conditions. The triple bend achromat lattice has been used mainly for small rings while on larger rings, its small dispersion value makes the chromaticity correction more difficult and the double bend achromat is usually preferred.

5 Perturbations

Up to now we have been considering a perfect machine, and in particular perfect magnetic fields, perfectly identical magnets and a perfect alignment on the reference trajectory. In practice, one now has to look at the detrimental effect of errors in all respects.

5.1 Resonances

We now introduce a single field error at one location. The motion turn after turn in the normalised phase space (X, X') is represented by circles (Figure 1.11). A particle initially perfectly centred experiences a kick $\Delta x'$ on each turn. For simplicity, we shall take the example of a dipolar error with an integer betatron tune.

For an exact integer tune, the amplitude will grow turn after turn until the particle is lost. If the tune differs slightly from the integer, after some time the kick will be out of phase with the particle oscillation and will start reducing the amplitude. The same applies to a quadrupolar

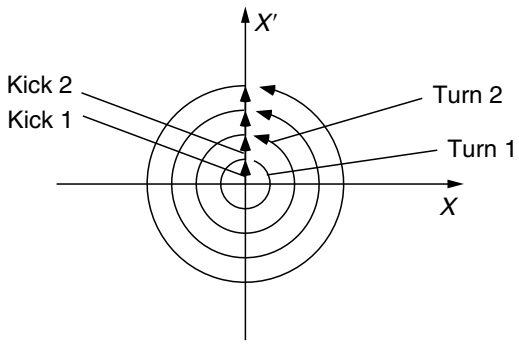

Figure 1.11 Resonant excitation.

kick and a half-integer tune and similarly to higher order multipolar fields and rational tune values. Generally speaking, a resonance line is defined by a line in the tune diagram (ν_x, ν_x) with equation

$$m\nu_x + n\nu_z = p$$

where $|m|+|n|$ is the order of the resonance, corresponding to $2(|m|+|n|)$-pole field errors and p is the harmonic number. When p is a multiple of the number of superperiods in the machine, the resonance is called systematic and is excited by the main magnetic fields of the structure (dipoles, quadrupoles, sextupoles, higher multipolar fields present in the magnets and so on). When p is not a multiple of the periodicity of the machine, the resonance is non-systematic and can only be excited by the non-identity between the superperiods (caused by magnet manufacturing tolerances, imperfect alignment and so on). Non-systematic resonances are usually much weaker than systematic ones.

The effect of resonance may be limited by:

- a choice of the working point (ν_x, ν_x) away from the lowest order resonances. It is also necessary to limit the tune spread, due, for instance, to the chromaticity and energy spread of the beam;
- for non-systematic resonances, powering a few corrector magnets may cancel the contribution of magnetic field errors to a given harmonic of a resonance and partially restore the periodicity of the structure;
- considering the radiation damping which acts against the invariant growth;
- getting Landau damping: when the betatron tune shifts as amplitude grows, because of non-linearities, the particle goes out of synchronism with the resonance.

5.2 Horizontal/vertical coupling

The initial assumption of the mid-plane symmetry of magnetic fields ensured a full decoupling of horizontal and vertical motions. Since the vertical equilibrium emittance is extremely small, the beam cross section should be a horizontal line. Practically a fraction of the horizontal motion transfers into the vertical direction. Several factors are involved:

- Betatron coupling: a tilted quadrupole bends vertically a particle horizontally off-centred. In such a case, a part of the horizontal motion is transferred into the vertical plane in such

a way that the sum of the emittances is preserved: $\varepsilon_x + \varepsilon_z = \varepsilon_0$. A coupling coefficient k is defined as

$$k = \varepsilon_z / \varepsilon_x \tag{52}$$

Powering skew quadrupole correctors can compensate this effect.

- Vertical dispersion: any vertical bending of the beam (resulting for instance from a tilt angle of dipole magnets) generates vertical dispersion. Consequently the synchrotron radiation emission excites a vertical betatron oscillation, as in the horizontal plane, and contributes to the vertical emittance.
- Coupling of the horizontal dispersion into the vertical plane: tilted quadrupoles at locations where the horizontal dispersion is non-zero also create vertical dispersion with the same consequences as above. This can also be used for correction by powering skew quadrupole correctors to try to cancel the spurious vertical dispersion.

5.3 Orbit distortions, beam stability

The reference trajectory is defined assuming perfect magnetic elements. In reality, unavoidable imperfections will cause the trajectory of the beam centre of mass (closed orbit) to deviate form this perfect orbit. The main errors come from

- transverse (horizontal or vertical) misalignment of quadrupoles.

Other errors have a smaller contribution:

- errors in bending magnet length or field;
- bending magnet tilt;
- misalignment of other elements (dipoles, sextupoles, etc.);
- magnetic field variations in the magnetic elements (fluctuations of power supplies or geometry modification following thermal effects);
- parasitic external magnetic fields.

All these errors generate an angular kick on the trajectory at the location of the error. The closed orbit distortion generated by a single kick can be easily computed: for instance, in the horizontal plane

$$\Delta x(s) = \frac{\Delta x'_{\text{kick}} \sqrt{\beta(s) \cdot \beta_{\text{kick}}}}{2 \cdot |\sin \pi \nu|} \cos\left(\pi \nu - |\varphi(s) - \varphi_{\text{kick}}|\right) \tag{53}$$

where $\beta_{\text{kick}}, \varphi_{\text{kick}}$ are optical functions at the kick location and

$$\Delta x'_{\text{kick}} = \frac{\Delta(B \cdot l)}{(p/e)}$$

is the angular kick generated by the integrated field error $\Delta(B \cdot l)$.

For several errors, one simply adds all the orbit distortions (assuming linear optics). For time-varying perturbations one can consider that the beam stabilises on the distorted closed orbit after a few damping times (typically a few milliseconds). Therefore, the centre of mass motion can be deduced from the perturbation behaviour using the static formula up to a few hundreds of Hertz.

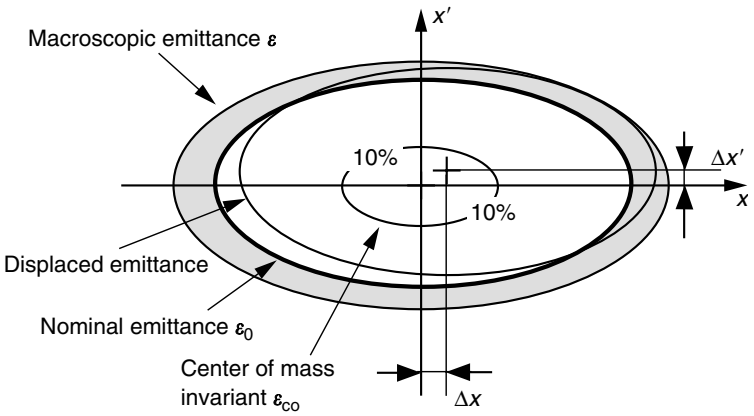

Figure 1.12 Macroscopic emittance growth.

At any point the perturbation can be measured by Δx, $\Delta x'$ and the degradation is quantified by relating this perturbation to the equilibrium beam size and divergence σ_x, $\sigma_{x'}$. This is done by introducing a 'macroscopic emittance growth', $\Delta\varepsilon/\varepsilon = (\varepsilon - \varepsilon_0)/\varepsilon_0$, envelope over a period of time of the instantaneous displaced emittances of the beam (Figure 1.12).

The emittance growth has the interesting properties that

- it is independent of the location along the circumference of the machine;
- it ensures a fair balance between position and angle errors all around the machine;
- it is also constant along a beam line for any drift space or focusing.

The emittance growth can be related to $\varepsilon_{\text{co}} = \gamma x_{\text{co}}^2 + 2\alpha x_{\text{co}} x'_{\text{co}} + \beta x'^2_{\text{co}}$, the Courant–Snyder invariant of the closed orbit, possibly time-dependent:

$$\frac{\Delta\varepsilon}{\varepsilon} = 2\sqrt{\frac{\varepsilon_{\text{co}}}{\varepsilon_0}} \tag{54}$$

5.4 Perturbations induced by insertion devices

The disturbance introduced by insertion devices results from two contributions:

- the perturbations resulting from a perfect insertion device;
- the effect of errors in the insertion device field.

In both cases the perturbation may be enhanced by the fact that the insertion device can be turned on or off at any time.

5.4.1 Perfect insertion device

A perfect insertion device induces the following:

- an additional focusing, consequently destroying the machine periodicity;
- higher order field components possibly exciting non-systematic resonances and reducing the dynamic aperture;

- a change in equilibrium emittance, in the case of a non-zero dispersion in the insertion device, or if the dispersion generated by the insertion device itself cannot be neglected.

The simplest approximation (Halbach's formula) for the field of an insertion device with period λ is given by

$$\begin{aligned} B_x &= (k_x/k_z) \cdot B_0 \cdot \sinh k_x x \cdot \sinh k_z z \cdot \cos ks \\ B_z &= B_0 \cdot \cosh k_x x \cdot \cosh k_z z \cdot \cos ks \\ B_s &= -(k/k_z) \cdot B_0 \cdot \cosh k_x x \cdot \sinh k_z z \cdot \sin ks \end{aligned} \tag{55}$$

where B_0 is the peak magnetic field, λ the period length and $k_x^2 + k_z^2 = k^2 = (2\pi/\lambda)^2$. k_x expresses the transverse variation of the field due to the limited pole width. It is zero for infinitely wide poles and is imaginary for standard insertion devices. The corresponding focusing strengths (see Eqn (7)) and tune shifts are then given by

$$\begin{aligned} K_x^2 &= \frac{k_x^2}{2k^2}\frac{B_0^2}{(p/e)^2} \qquad \Delta\nu_x = \frac{k_x^2}{8\pi k^2}\frac{B_0^2}{(p/e)^2}L \\ K_z^2 &= \frac{k_z^2}{2k^2}\frac{B_0^2}{(p/e)^2} \qquad \Delta\nu_z = \frac{k_z^2}{8\pi k^2}\frac{B_0^2}{(p/e)^2}L \end{aligned} \tag{56}$$

where L is the total length of the insertion device. The focusing effect is independent of the period length λ, and in the simple case $k_x = 0, k_z = k$, it is null in the horizontal plane. This simple field approximation is valid far away from the pole surfaces but generally gives a poor approximation for realistic insertion devices. However, it describes the main effect of a perfect insertion device: a focusing effect, mainly in the vertical plane, inversely proportional to the square of the momentum. This focusing effect is noticeable on low-energy machines, but can be negligible on high-energy storage rings. The same scaling applies to higher order multipolar fields.

A more general field distribution can be studied [1] in the following approximations:

1 The field integrals in both planes are vanishing over the insertion device:

$$\int_{-\infty}^{\infty} B_x \, \mathrm{d}s = 0 \qquad \int_{-\infty}^{\infty} B_z \, \mathrm{d}s = 0 \tag{57}$$

2 The double field integrals in both planes are also vanishing over the insertion device:

$$\int_{-\infty}^{\infty}\int_{-\infty}^{s} B_x \, \mathrm{d}s' \, \mathrm{d}s = 0 \qquad \int_{-\infty}^{\infty}\int_{-\infty}^{s} B_z \, \mathrm{d}s' \, \mathrm{d}s = 0 \tag{58}$$

These conditions express the basic properties of an insertion device: the field integral should not induce any angle or any displacement of the reference trajectory. We will add the additional approximation that the initial horizontal and vertical angles of the trajectory are zero or

extremely small:

$$x'(-\infty) = z'(-\infty) \approx 0$$

Then the angles of the trajectory at the exit of the insertion device are given by:

$$\begin{aligned} x'(\infty) &= -\frac{1}{2(p/e)^2}\int_{-\infty}^{\infty}\frac{\partial}{\partial x}\Phi(x,z,s)\,\mathrm{d}s + o\left(\frac{1}{(p/e)^3}\right) \\ z'(\infty) &= -\frac{1}{2(p/e)^2}\int_{-\infty}^{\infty}\frac{\partial}{\partial z}\Phi(x,z,s)\,\mathrm{d}s + o\left(\frac{1}{(p/e)^3}\right) \end{aligned} \tag{59}$$

The angular kicks experienced by the particle are derived from the function

$$\Phi(x,z,s) = \left(\int_{-\infty}^{s} B_x\,\mathrm{d}s'\right)^2 + \left(\int_{-\infty}^{s} B_z\,\mathrm{d}s'\right)^2 \tag{60}$$

As usual insertion devices are periodic, the function Φ can be integrated over one period, resulting in a potential U given by

$$U(x,z) = \int_{1\text{ period}} \Phi(x,z,s)\,\mathrm{d}s \tag{61}$$

The angular kick experienced by a particle over the undulator period is then

$$\begin{aligned} \Delta x' &= -\frac{1}{2(p/e)^2}\frac{\partial U}{\partial x}(x,z) \\ \Delta z' &= -\frac{1}{2(p/e)^2}\frac{\partial U}{\partial z}(x,z) \end{aligned} \tag{62}$$

In the ideal case of the analytical field expansion (Eqn (55)), this potential expression gives again the main focusing effect. But the potential U can be obtained for any kind of insertion device, either from magnetic field computations or from magnetic measurements.

5.4.2 Field errors

In the previous paragraph we assumed that the insertion device restores at its end both:

- the beam angle:

$$\int_{-\infty}^{\infty} B_{x,z}\,\mathrm{d}s = 0$$

- the beam position:

$$\iint B_{x,z}\,\mathrm{d}s\,\mathrm{d}s' = 0$$

In practice, this is not exactly true because of imperfections. The construction errors can be minimised using shimming techniques. The difficulty is increased by the fact that these conditions must be fulfilled for any tuning of the insertion device. Residual errors can be compensated by powering correcting magnets at each end of the insertion device.

6 Collective effects

We can now look at what happens when we try to increase the intensity in the storage ring: at some point we can no longer consider that particles ignore each other. As particles are relativistic the space charge effect vanishes completely, but one has to take into account the fact that the beam has to be surrounded by a vacuum chamber built with conducting material. Electromagnetic fields will develop in this volume and possibly interact with the beam itself. This will lead to instability if any perturbation in the particle density grows exponentially.

As the particle density in the bunch grows, the probability of interaction between particles increases. Multiple scattering between particles, called 'intrabeam scattering' will modify the equilibrium emittance of the beam and prevent it from reaching extremely small emittances.

These effects appear in many different ways: longitudinal or transverse direction, single bunch or multibunch operation. They are responsible for the intensity (and brightness) limitation of synchrotron radiation sources.

6.1 Interaction with the vacuum chamber

The first step is to look at the electromagnetic field created by a single electric charge travelling at the velocity of light in a conductive beam pipe. We can split the problem by studying first the longitudinal field (considering a particle along the axis of a cylindrically symmetrical pipe) and then the transverse field (null as long as the particle is centred but varying with its transverse position).

6.1.1 Longitudinal wake field

The Green's function is obtained by integrating the longitudinal electric field seen at a fixed distance (or delay τ) behind a single punctual charge q. It corresponds to a longitudinal accelerating (or decelerating) voltage seen by a test particle following the charge q over one turn, per unit charge:

$$G_{\parallel}(\tau) = -\frac{1}{q}\int_C E_{\parallel}\left(s, t = \frac{s}{\beta c} + \tau\right) \mathrm{d}s \tag{63}$$

This quantity completely defines the influence of the environment on the test particle. Usually it cannot be computed analytically for real vacuum chamber geometry but it can be estimated with computer codes. The total accelerating voltage (called 'wake potential') resulting from a real beam, knowing the particle line density $\lambda(\tau)$ and the total charge of the bunch Q, can be obtained by integration:

$$W_{\parallel}(\tau) = -Q \cdot \int_{-\infty}^{\infty} G(\tau - \tau')\lambda(\tau')\mathrm{d}\tau' \tag{64}$$

Going to the frequency domain, the convolution of the beam line density with the Green's function is transformed into the product

$$W_{\parallel}(\omega) = -I(\omega) \cdot Z_{\parallel}(\omega) \tag{65}$$

which suggests the definition of the coupling impedance Z:

$$Z_{\parallel}(\omega) = \int_{-\infty}^{\infty} G_{\parallel}(\tau)\, \mathrm{e}^{-\mathrm{j}\omega\tau}\, \mathrm{d}\tau \quad \text{(longitudinal coupling impedance)} \tag{66}$$

$$I(\omega) = Q \int_{-\infty}^{\infty} \lambda(\tau)\, \mathrm{e}^{-\mathrm{j}\omega\tau}\, \mathrm{d}\tau \quad \text{(beam intensity)} \tag{67}$$

The wake potential $W_{\parallel}(\tau)$ can be considered as a perturbation to be added to the accelerating voltage provided by the RF system. In a perfectly conducting cylindrical vacuum chamber, the wake field would be null. The main contributions to the impedance come from:

Resistive wall: The resistance seen by the image charge circulating in the vacuum chamber creates a longitudinal electric field component on the beam axis.

High-Q resonators: The objects are typically the accelerating RF cavities, with their fundamental mode and possibly higher order mode (HOM). The wake field generated there extends over a long period so that it can affect several consecutive bunches. High-Q resonators are involved in multibunch instabilities.

Broadband resonator: All the discontinuities of the cross section of the vacuum chamber can be cumulated in a broadband resonator (usually $Q = 1$) summarising their effect:

$$Z_{\parallel \mathrm{BB}}(\omega) = \frac{R_{\mathrm{s}}}{1 + \mathrm{j}Q((\omega/\omega_r) - (\omega_r/\omega))} \tag{68}$$

The resonance frequency ω_r is related to the vacuum chamber radius. The influence of a broadband resonator is limited to very short-term: the field generated by the head of the bunch influences its tail but disappears before the next bunch. It is mainly involved in single bunch instabilities.

The quantity of interest in longitudinal instabilities is in fact $Z(\omega)/\omega$ or even better $Z(p)/p$, with p a harmonic of the revolution frequency: $p = \omega/\omega_0$. Figure 1.13 shows the main contributions to the impedance.

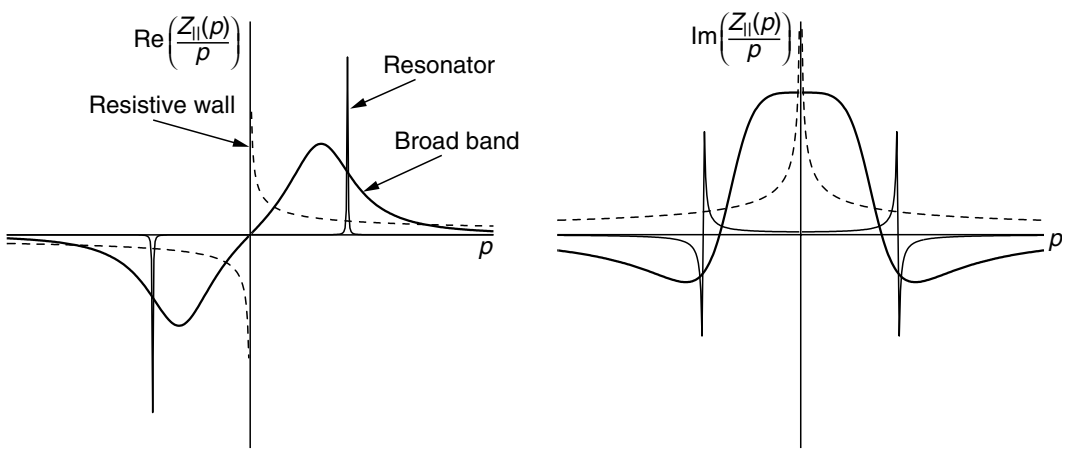

Figure 1.13 Longitudinal impedance spectrum.

6.1.2 Beam signal

It appears now that the perturbation seen by a particle is the consequence of the interaction between the beam spectrum and the coupling impedance of the machine. Therefore, we need to express in the frequency domain the signal created by a circulating unperturbed (Gaussian) beam, followed by the signal created by any perturbation of this distribution. Instability will occur if the spectrum of a perturbation interacts with the impedance so that the perturbation amplitude grows. Longitudinally the signal of a stationary Gaussian bunch is a line spectrum at multiples of the revolution frequency:

$$S_{\parallel}(\omega = p\omega_0) = I \sum_p \delta(\omega - p\omega_0) \exp\left(-\frac{p^2\omega_0^2\sigma_\tau^2}{2}\right) \tag{69}$$

The envelope of the spectrum extends up to a frequency $1/\sigma_\tau$. This frequency is usually similar to the resonance frequency of the broadband impedance of the vacuum chamber. The interaction occurs mainly with the inductive part of the resonator. This is why the coupling impedance is sometimes described only by the inductance value.

Perturbations may be added to this distribution. They can be expressed as a combination of modes defined in the following way:

- Mode 1 corresponds to a global oscillation of the bunch in phase and in energy around its equilibrium position at a frequency Ω_s.
- Mode 2 is an oscillation of the bunch length and energy spread at frequency $2\Omega_s$.

The spectrum of mode m shows sidebands at frequency $m\Omega_s$ apart from each harmonic of the revolution frequency $p\omega_0$. Figure 1.14 shows the spectrum of the stationary distribution and of modes 1 and 2 in the absence of influence of the self-induced field. It is plotted as on a real spectrum analyser with negative frequencies folded over positive ones. For multibunch perturbations, each mode is subdivided into sub-modes differing by the phase difference between successive bunches.

6.1.3 Longitudinal instabilities

The interaction between the bunch spectrum and the real part of the coupling impedance creates power dissipation and an asymmetry of the bunch longitudinal profile. The interaction with the imaginary part creates a shift of synchrotron frequency and bunch lengthening (or shortening).

Power dissipation: The interaction with the resistive part of the impedance creates losses: Equation (64) gives the energy loss for the test particle. Integrating over the whole bunch gives the energy loss for the bunch. This shows a Q^2, square of the bunch charge. The total energy loss can be expressed as $\Delta E = -k_{\mathrm{LOSS}} \cdot Q^2$, where k the 'loss factor' is

$$k_{\mathrm{LOSS}} = \frac{1}{2\pi} \int_{-\infty}^{\infty} \mathrm{Re}(Z(\omega))|\lambda(\omega)|^2 \, \mathrm{d}\omega \tag{70}$$

The losses depend on the bunch line density λ: a short bunch extends higher in frequency and creates more losses. The synchronous phase is shifted so that the losses are restored by the RF system.

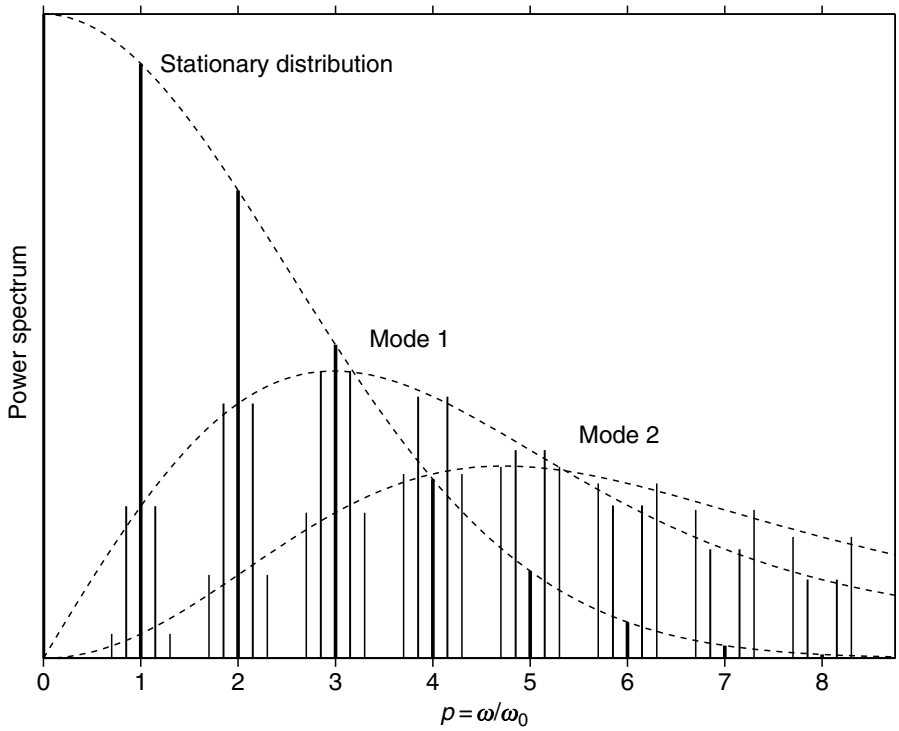

Figure 1.14 Longitudinal beam spectrum.

Potential well distortion: The imaginary part of the impedance (inductance over the lower frequency range and capacitance above the resonance frequency) creates a voltage over the bunch length that modifies the voltage created by the accelerating cavity. Consequently, the stationary distribution of particles will be modified as will the incoherent synchrotron frequency, synchronous phase and bunch length. For realistic impedances, this results in a bunch lengthening for $\eta_C < 0$ or shortening for $\eta_C > 0$, with a constant energy distribution. This will happen up to a threshold corresponding to an infinite or vanishing RF voltage slope. Above this threshold, the energy spread of the bunch will grow while the bunch lengthens. According to Equation (46), the bunch length can be reduced at zero current by reducing η_C. However, the lengthening due to the longitudinal coupling impedance gives a lower limit, function of the beam current but independent of η_C, for the minimum bunch length [2].

Coupled bunch instabilities: High-Q resonators, like higher order modes of accelerating cavities may induce wake fields which couple adjacent bunches in multibunch operation. In such cases, the impedance is narrow band while the spacing between the lines of the beam spectrum is increased by the number of bunches. It may then be possible to tune the resonators so that they do not interfere with the beam.

6.1.4 Transverse wake field

If the beam is displaced from the axis of a symmetrical vacuum chamber, the electromagnetic induced fields also have a transverse component. Among the numerous azimuthal modes, one considers only the lowest one, the dipole mode, the strength of which is proportional to the displacement Δ of the beam. This mode gives a deflection of the whole beam and may

generate coherent transverse oscillations of the beam centre of mass. Following what was done for longitudinal direction, we define a transverse Green function based on the integral of the deflecting force seen by a test particle following the reference particle, both off-centred by an offset Δ:

$$G_\perp(\tau) = \frac{1}{q\Delta\beta}\int_C (E + \beta c B)_\perp \left(s, t = \frac{s}{\beta c} + \tau\right) \mathrm{d}s \tag{71}$$

The beam signal ('transverse intensity') is defined as the product of the beam transverse position by its intensity, as it can be measured on an ideal beam position monitor. The perturbation is now the deflecting force, proportional to the elongation Δ and integrated over one turn. This adds to the focusing provided by the quadrupoles. The transverse coupling impedance is defined as:

$$Z_\perp(\omega) = \mathrm{j}\int_{-\infty}^{\infty} G_\perp(\tau)\,\mathrm{e}^{-\mathrm{j}\omega\tau}\,\mathrm{d}\tau \tag{72}$$

6.1.5 Transverse impedance

Impedance contributions are the same as for longitudinal direction. For simple cylindrical geometry with radius b, the transverse impedance is linked to the longitudinal impedance by the simple formula

$$Z_\perp(\omega) = \frac{2c}{b^2}\frac{Z_\parallel(\omega)}{\omega} \tag{73}$$

6.1.6 Transverse beam signal

The unperturbed beam is on-axis and consequently the signal from the stationary distribution is null. Only perturbations contribute to the transverse signal of the beam. We define perturbation modes as the following:

- mode 0 in a global transverse oscillation of the whole bunch;
- mode 1 shows opposite oscillation amplitude at the head and tail of the bunch (1 node over the bunch length).

More generally mode m has m nodes over the bunch length and its spectrum has lines at frequencies $(p + \nu)\omega_0 + m\Omega_\mathrm{s}$. The symmetry point of the envelopes of all these modes is shifted from the zero frequency by a value ω_ξ depending on the chromaticity (Figure 1.15):

$$\omega_\xi = \nu\omega_0\frac{\xi}{\eta_\mathrm{C}} \tag{74}$$

6.1.7 Transverse instabilities

The interaction of the beam spectrum with the imaginary part of the impedance produces tune shifts while the interaction with the real part gives damping or anti-damping. As suggested by Eqn (73), the transverse impedance spectrum is similar to the longitudinal one.

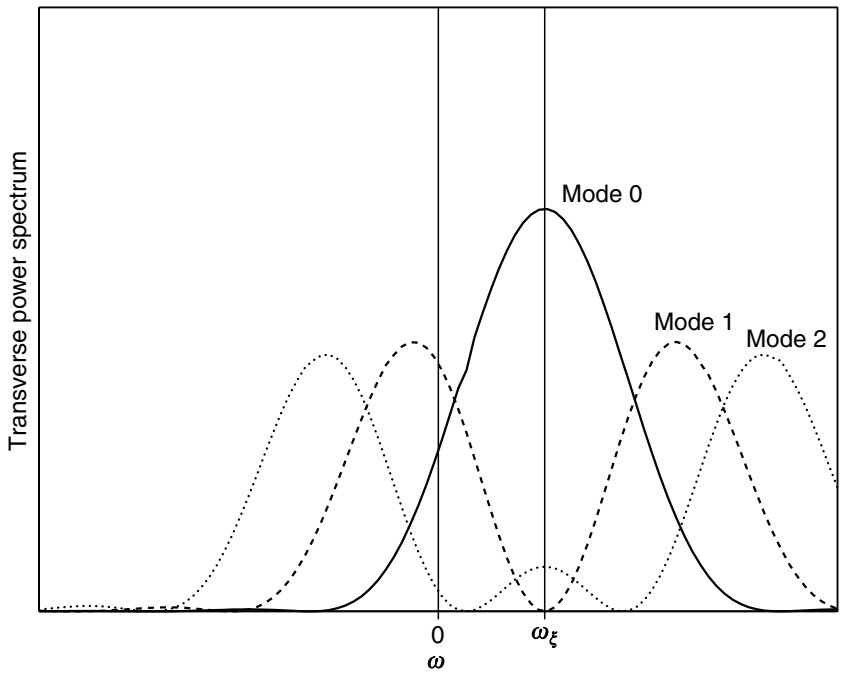

Figure 1.15 Envelope of transverse spectrum.

Tune shifts: The interaction of the spectrum of mode 0 (rigid transverse oscillation of the bunch) with the imaginary part of the transverse impedance adds to the focusing effect of the main quadrupoles. This results in a coherent tune shift proportional to the bunch intensity. This can be seen mainly in single bunch operation.

Head-tail instability: The wake field generated by the head of the bunch creates a deflecting force on the tail. At the same time the longitudinal oscillation within the bunch interchanges the particles between head and tail and modifies their transverse oscillation frequency through the chromaticity. This leads to a current threshold above which the coherent motion of the bunch is anti-damped. However, since a variation of chromaticity displaces the envelope of the different transverse coherent modes, it is possible to raise these thresholds by moving the most dangerous modes with respect to the real part of the impedance.

6.2 Intrabeam scattering

As the particle density in the bunches increases, the probability of collisions between particles becomes greater. If the number of collisions with small exchanges of momentum during a damping time is large, it causes a significant change in the equilibrium distribution. Without taking into account the radiation damping, this would correspond to a modification of the sharing of oscillation energies between the three planes, satisfying the relation

$$a \cdot \sigma_\delta^2 \eta_C + b \cdot \nu_x \varepsilon_x + c \cdot \nu_z \varepsilon_z = \text{constant} \tag{75}$$

where a, b, c are constants depending on the lattice.

The behaviour depends on the sign of η_C. For $\eta_C < 0$, as it is for most synchrotron radiation sources, the three invariants may grow indefinitely, taking energy from the RF system. The growth rates of the invariants have to be compared with the radiation damping times. They are inversely proportional to a density factor A involving the six-dimensional volume of the bunch:

$$A = \frac{r_e^2 c N}{64\pi^2 \sigma_s \sigma_\delta \sigma_x \sigma_y \sigma_{x'} \sigma_{z'} \beta^3 \gamma^4} \tag{76}$$

The energy dependence in $\beta^3\gamma^4$ indicates that the effect mostly affects low energy machines. The theoretical minimum emittance values given in Eqns (49)–(51) suggest that one could reduce the emittance to any desired value by increasing the machine dimensions. Intra-beam scattering gives an absolute lower limitation of the emittances, at least for reasonable intensities.

7 Beam lifetime

The distribution of the particles in phase space, resulting from the equilibrium between synchrotron radiation and damping is Gaussian. However, it has to be modified to take into account the longitudinal or transverse limitations of the oscillation amplitudes. In addition, other effects may contribute to the excitation of oscillations. This leads to a rate of loss of particles expressed as the beam lifetime τ so that:

$$\frac{1}{\tau} = -\frac{1}{I}\frac{\mathrm{d}I}{\mathrm{d}t} \tag{77}$$

Different loss processes will be shown and the resulting lifetime will be the combination of all effects given by

$$\frac{1}{\tau} = \sum_i \frac{1}{\tau_i} \tag{78}$$

When computing lifetimes we shall refer to the different acceptance values defined in Section 4.2: ε_m the transverse acceptance (x or z) and δ_m the momentum acceptance.

7.1 Quantum lifetime

The stationary distribution of particles is deduced from the Fokker–Planck equation. In Section 4.4, we computed the distribution for an infinitely wide aperture. A correction must be added to match the boundary condition that the particle density must be zero at the limit of aperture. The resulting lifetime for a limitation in one plane (x, z or δ) is:

$$\frac{1}{\tau_q} = \frac{r_{x,z,\delta}}{\tau_{x,z,\delta}} \exp\left(-\frac{r_{x,z,\delta}}{2}\right) \tag{79}$$

where $\tau_{x,z,\delta}$ is the damping time in the considered plane and $r_{x,z,\delta}$ is the relative aperture:

$$r_{x,z} = \frac{\varepsilon_m}{\varepsilon_{x,z}} = \left(\frac{x_m, z_m}{\sigma_{x,z}}\right)^2 \qquad r_\delta = \frac{\delta_m^2}{\sigma_\delta^2}$$

This contribution to the lifetime is only significant for very small apertures. One usually considers that it can be neglected when the aperture is larger than six standard deviations of the beam size.

7.2 Coulomb scattering

This is a part of the interaction of the circulating particles with the residual gas in the vacuum chamber. We consider elastic scattering of a particle interacting with the nucleus of an atom of the residual gas. We restrict ourselves to angles large enough so that the particle gets out of the transverse acceptance of the machine. The differential cross section for Coulomb scattering is given by the Rutherford formula:

$$\frac{\mathrm{d}\sigma}{\mathrm{d}\Omega} = \left(\frac{r_\mathrm{e} Z}{2\gamma\beta^2}\right)^2 \frac{1}{\sin^4(\theta/2)} \tag{80}$$

where θ is the scattering angle, Z the charge of the nucleus and r_e the classical electron radius: $r_\mathrm{e} = 2.82 \cdot 10^{-15}$ m.

This cross section has to be integrated over all scattering angles larger than the transverse angular acceptance of the machine $\varepsilon_\mathrm{m}/\beta$. Usually, the angular acceptance in storage rings is smaller in the vertical plane, because of constraints in magnet and insertion device gaps. If we neglect the limitation in the horizontal plane, we get

$$\sigma = 2\pi \left(\frac{r_\mathrm{e} Z}{\gamma\beta^2}\right)^2 \frac{\beta_z}{\varepsilon_\mathrm{m}} \tag{81}$$

The lifetime is then obtained by combining the effect of all components of the residual gas and integrating over the circumference:

$$\frac{1}{\tau_\mathrm{sc}} = \frac{2\pi r_\mathrm{e}^2 c}{\gamma^2\beta^3 kT} \frac{1}{\varepsilon_\mathrm{m}} \sum_{\mathrm{atom}\, j} \left(Z_j^2 \sum_{\mathrm{gas}\ i} \alpha_{ij} \langle \beta_z p_i \rangle \right) \tag{82}$$

where α_{ij} is the number of atoms j per molecule i, p_i the partial pressure of gas i, Z_j the charge of atom j, k the Boltzmann constant ($k = 1.38 \cdot 10^{-23}$ J/K), T the absolute temperature and r_e the classical electron radius defined above.

The Coulomb scattering lifetime depends strongly on the electron energy (γ^{-2}) and on the transverse aperture of the machine. In case the pressure and β functions vary along the circumference, it is important to have a low pressure where β is large.

7.3 Bremsstrahlung

Here we look at inelastic scattering of the particles on the residual gas. The loss is due to the longitudinal acceptance of the machine. The differential cross section for an energy loss

between E_b and $E_\mathrm{b} + \mathrm{d}E_\mathrm{b}$ is given by:

$$\mathrm{d}\sigma = \frac{4r_\mathrm{e}^2 Z^2}{137} F(E, E_\mathrm{b}) \frac{\mathrm{d}E_\mathrm{b}}{E_\mathrm{b}} \tag{83}$$

For high-energy electrons, the function F is given approximately by the Bethe–Heitler formula:

$$F(E, E_\mathrm{b}) = \left[\frac{4}{3} \left(1 - \frac{E_\mathrm{b}}{E} \right) + \left(\frac{E_\mathrm{b}}{E} \right)^2 \right] \ln \frac{183}{Z^{1/3}} + \frac{1}{9} \left(1 - \frac{E_\mathrm{b}}{E} \right) \tag{84}$$

This cross section has to be integrated between the energy acceptance of the machine E_m and infinity, and then integrated over the circumference of the machine. With some approximations the result is

$$\frac{1}{\tau_\mathrm{b}} = \frac{4r_\mathrm{e}^2 c}{137\, kT} \left(\frac{4}{3} \ln \frac{1}{\delta_\mathrm{m}} - \frac{5}{6} \right) \sum_{\text{atom } j} \left(Z_j^2 \ln \frac{183}{Z_j^{1/3}} \sum_{\text{gas } i} \alpha_{ij}\, p_i \right) \tag{85}$$

The Bremsstrahlung lifetime is roughly independent of energy. It is limited by the momentum acceptance of the machine. In similar conditions a low-energy machine is more sensitive to Coulomb scattering while a higher energy machine is dominated by Bremsstrahlung.

7.4 Touschek effect

For large intensities, the particle density in the bunch becomes large. As particles are oscillating independently inside the bunch, the probability of collisions between particles increases and may result in particle loss. The longitudinal oscillation frequency is usually much smaller than the transverse ones: in the bunch frame, the oscillation energy is larger in the transverse planes than in the longitudinal plane. A collision thus mainly transfers transverse energy into the longitudinal plane. Moreover, in the case of synchrotron radiation sources the horizontal beam size is much larger than the vertical one, so that we can restrict ourselves to the simple case of collisions transferring horizontal motion into the longitudinal direction.

In the referential defined by the centre of mass of the two colliding particles, the differential cross section is given by the Möller formula:

$$\frac{\mathrm{d}\bar{\sigma}}{\mathrm{d}\Omega} = \frac{r_\mathrm{e}^2}{4\bar{\beta}^4} \left(\frac{4}{\sin^4 \theta} - \frac{3}{\sin^2 \theta} \right) \tag{86}$$

where $\bar{\sigma}$ is the cross section in the centre of mass frame and $\bar{\beta}$ the relative velocity of each particle in the centre of mass frame, supposed non-relativistic ($\bar{\beta} \ll 1$).